Proceedings of ASME Turbo Expo 2011
GT2011
June 6-10, 2011, Vancouver, British Columbia, Canada

GT2011-45961

THERMAL ANALYSIS OF COOLING SYSTEM IN A GAS TURBINE TRANSITION PIECE

Jun Su Park[a], Namgeon Yun [a], Hokyu Moon [a], Kyung Min Kim [a], Sin-Ho Kang[b] and Hyung Hee Cho [a†]

[a] Department of Mechanical Engineering, Yonsei University, Seoul, 120-749, Korea
E-mail: hhcho@yonsei.ac.kr

[b] Korea Plant Service Engineering Co. Incheon, 404-718, Korea

ABSTRACT

This paper presents thermal analyses of the cooling system of a transition piece, which is one of the primary hot components in a gas turbine engine. The thermal analyses include heat transfer distributions induced by heat and fluid flow, temperature, and thermal stresses. The purpose of this study is to provide basic thermal and structural information on transition piece, to facilitate their maintenance and repair. The study is carried out primarily by numerical methods, using the commercial software, Fluent and ANSYS. First, the combustion field in a combustion liner with nine fuel nozzles is analyzed to determine the inlet conditions of a transition piece. Using the results of this analysis, pressure distributions inside a transition piece are calculated. The outside of the transition piece in a dump diffuser system is also analyzed. Information on the pressure differences is then used to obtain data on cooling channel flow (one of the methods for cooling a transition piece). The cooling channels have exit holes that function as film-cooling holes. Thermal and flow analyses are carried out on the inside of a film-cooled transition piece. The results are used to investigate the adjacent temperatures and wall heat transfer coefficients inside the transition piece. Overall temperature and thermal stress distributions of the transition piece are obtained. These results will provide a direction to improve thermal design of transition piece.

Key words: Gas turbine, Combustor, Transition piece, Film cooling, Thermal stress.

INTRODUCTION

The combustor of a gas turbine is exposed to hot combustion gas. Components of the combustor, including the combustion basket (liner) and transition piece, experience high thermal loads, and the combustor surfaces have a non-uniform heat transfer distribution. This non-uniform heat transfer distribution causes high thermal stress variation, reducing the durability and efficiency of the combustor. To address this, a suitable cooling system is required. However, previous studies have mostly focused on combustion analysis, and have not considered the heat transfer or thermal stresses on the components of a combustor.

Kim et al. [1] conducted a numerical study of the combustion flame in a lean-burn combustor to reduce NOx emissions. They analyzed the combustion flame using the LES model, and confirmed that the results were in agreement with those obtained from experiments. Chung et al. [2] used the commercial software Fluent to carry out flow pattern analysis in the combustion liner and transition piece of the 7FA model. Kang et al. [3] investigated combustion and flame stability in lean premixed combustion, comparing numerical and experimental results.

Agrawal et al. [4] modeled a dump diffuser and components close to the combustion for a land-based gas turbine. They investigated flow characteristics experimentally and numerically in the dump diffuser and near the outside of the combustor. Bailey et al. [5] studied the cooling system of a combustion liner. This system consisted of the combustion liner and a flow sleeve, and impinging jet and internal passage cooling were used. Heat transfer was measured on the outside surface of the combustion liner. Mustafa et al. [6] calculated the distribution of thermal stresses on a simplified transition piece. They also considered real material properties.

Much information is currently available on the relationship between combustion and the distribution of heat transfer in the simplified models. However, there are limitations on improving the durability and efficiency. It is thus necessary to study the flow pattern and cooling system in a full-sized combustor.

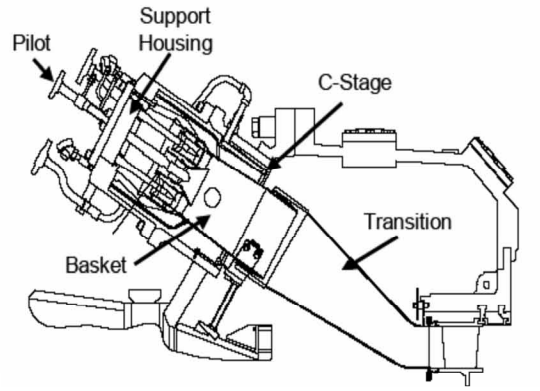

Figure 1. Components of the combustor

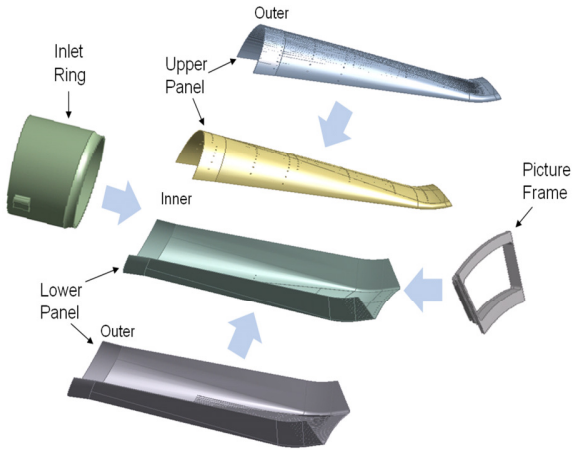

Figure 2. Components of the transition piece

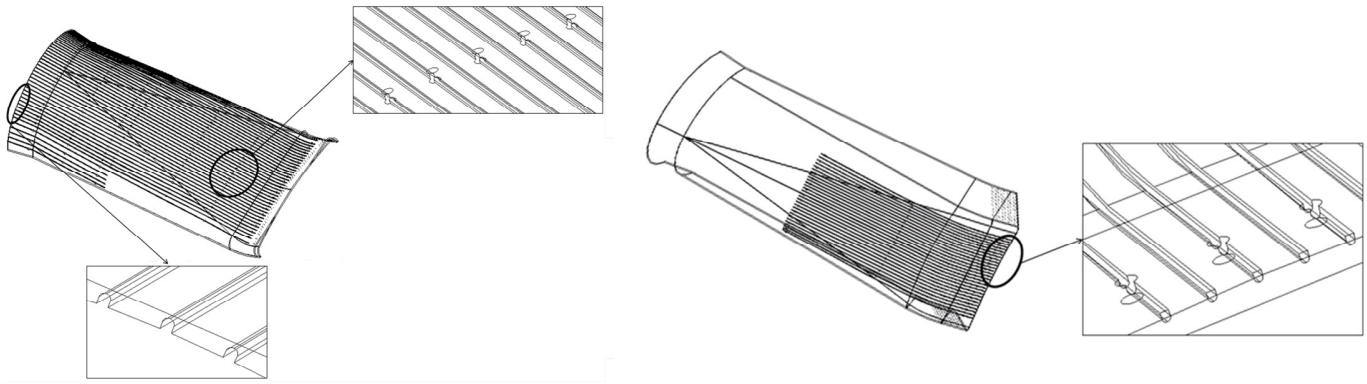

(a) Layout of the upper panel

(b) Layout of the lower panel

Figure 3. Modeling of the cooling channel on upper and lower panel

Thermal stress analysis and thermal design are also required to improve the durability and efficiency. The primary objective of this study is thermal analysis, and thermal damage to the transition piece is predicted. The combustion basket, transition piece with cooling system, and dump diffuser are modeled numerically, using the commercial software, Fluent and ANSYS. The results will be useful in designing a cooling system, and the operation and maintenance of an actual transition piece.

RESEARCH METHOD

Structure of the Combustor

Figure 1 shows the components of the combustor, including the combustion basket (liner), transition piece, and dump diffuser. The transition piece is connected to the combustion basket and the first vane row. Hot gas from the combustion basket passes through the transition piece and enters the first vane row. The cross-sectional shape of the transition piece changes from a circle to a quadrangle. This helps to create a uniform temperature distribution in the outlet of the transition piece.

Figures 2 and 3 show the components of the transition piece, which consists of upper and lower panels having three layers, such as outer, middle and inner layers. The outer and inner layers of the panels have holes in them. The holes in the outer layer are cooling air inlet holes, and the holes in the inner layer are outlet holes. Parts of the middle layer of the panels are removed to create the cooling channels. The cooling channels in the middle layer connect the cooling air inlet and outlet holes in the outer and inner layers, respectively. The cooling air passes from the dump diffuser to the inlet holes, through the cooling channels, and into the transition piece, directly protecting the inside wall of the transition piece from the hot combustion gas.

The combustion basket is a partially premixed combustor with one spread flame nozzle and eight premixed fuel nozzles. The spread flame nozzle is located at the center of combustor, and the eight premixed fuel nozzles surround the spread flame nozzle.

Numerical Calculations

To compute the thermal stresses, the distributions of the wall adjacent temperatures and wall heat transfer coefficients must first be calculated from information on heat and flow characteristics. The wall adjacent temperature is the gas temperature at the nearest grid points on the wall surface. It is difficult to experimentally obtain wall adjacent temperatures and wall heat transfer coefficients in a high temperature and pressure environment. Thus, the present study is based on a numerical analysis of the heat and flow characteristics of hot combustion gas inside a transition piece, and compressed air between the outside of the transition piece and the dump diffuser, using the commercial CFD software Fluent. Applying the CFD results, the temperature and stress distributions on the wall of the transition piece are calculated using the FEA software ANSYS.

The thermal analysis of the transition piece is divided into six steps:

1) Combustor analysis in the combustion basket.
2) Inside and outside flow analysis in the transition piece without film cooling.
3) Heat and flow analysis in the cooling channel.
4) Heat and flow analysis in the transition piece with film cooling.
5) Calculating the wall temperature and thermal stress on the transition piece.
6) Life prediction of the transition piece.

Modeling the Combustion Basket

The combustion basket (liner) is modeled to obtain the initial conditions. The outlet results for the combustion basket are used as the inlet conditions for the transition piece. The grid of the combustion basket was generated using GAMBIT, and consists of approximately 2.24 million cells. The calculation domain, ranging from the nozzle cap assembly to the end of the combustion basket, is 418 mm. The inner diameter of the nozzle cap is 279 mm, and that of the combustion basket connection with the transition piece is 287 mm. For the base-load operating conditions, the fuel gas is assumed to be CH_4, the dominant component of natural gas. The mass flow rate of the gas is 0.60 kg/s, and that of the compressed air is 24.0 kg/s. The equivalence ratio is 0.533, the average pressure in the combustion basket is 15.4 atm, and the fuel temperature at the nozzle inlet is 667K. The turbulence and species model are the realizable k-ε model and species transport, respectively. The species transport model deals mixing and transport of chemical species by solving conservation equations describing convection, diffusion, and reaction sources for each component of species. The combustion process is modeled by the following reaction:

$$CH_4 + 2(O_2+3.76N_2) \rightarrow CO_2 + 2H_2O + 7.52N_2 \qquad (1)$$

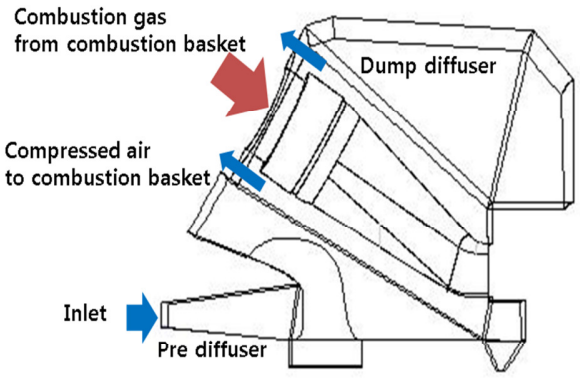

Figure 4. Modeling of the pre and dump diffuser

Modeling the Transition Piece

The inside and outside pressure distributions on the walls of the transition piece are calculated to obtain the mass flow rate in the cooling channel of the transition piece. The mass flow of the cooling air is calculated using the pressure differences between the inside and outside walls of the transition piece.

First, the transition piece is modeled to obtain the pressure distribution on its inside surfaces. The outlet of the combustion basket is inserted into the transition piece. The present model omits the cooling holes in the walls of the transition piece. The grid consists of 0.83 million cells. The inlet conditions are the velocity and temperature profiles from the outlet of the combustion basket. The realizable k-ε model and the standard wall function are used for the turbulent flow in the transition piece.

Second, the pre-diffuser and dump diffuser are modeled to calculate the pressure distribution on the outer surfaces of the transition piece. The combined volume of the combustion basket and transition piece is removed from the dump diffuser. The model of the pre-diffuser and dump diffuser employs the symmetry condition for 3D flow analysis. Figure 4 shows the model for the pre-diffuser and dump diffuser. The calculation ranges of the height and length from the pre-diffuser to the end of the transition piece are 1630 mm and 1150 mm, respectively. The number of total grid cells is 3.49 million. The pressure and temperature of the compressed air from the pre-diffuser are 15.4 atm and 667K, respectively. The mass flow of the compressed air is 12.0 kg/s. The realizable k-ε model and the standard wall function are used for the turbulent flow in the pre-diffuser and dump diffuser.

Third, the cooling channels in the transition piece are modeled. The upper panel has a total of 47 lines for the cooling channels, 39 with length 700 mm and eight with length 300 mm. Each of the long cooling channels has three or four cooling holes, while the short cooling channels have one or two. The lower panel has 29 lines for the cooling channels. All lines have a length of 500 mm and one or two cooling holes. The diameter of each cooling hole is 4 mm. The outer layer of

Table 1 Physical properties of Inconel 617 [8]

Temperature [℃]	Thermal Conductivity [W/m-℃]	Thermal Expansion Coefficient [μm/m-℃]	Young's Modulus [GPa]	Poisson's Ratio
100	14.7	11.6	206	0.30
200	16.3	12.6	201	0.30
400	19.3	13.6	188	0.30
600	22.5	14.0	173	0.30
800	25.5	15.4	157	0.30
1000	28.7	16.3	139	0.31

upper panel has 147 cooling holes, and 142 in the inner layer of upper panel. The outer layer of lower panel has 44 cooling holes, and 43 in the inner layer of lower panel. The width and height of the cooling channels are 1.65 mm and 2 mm, respectively, for both panels. For the sake of computational convenience, symmetry conditions are used in the analysis of the cooling channels. Thus, only 24 channels are modeled in the upper panel, and 15 channels in the lower panel. Each channel has approximately 0.13 million grid cells. The total number of grid cells in the cooling channels is 2.89 million for the upper panel, and 2.00 million for the lower panel. Figure 3 shows the modeling of the cooling channels in the upper and lower panels. The temperature of the cooling air is 667K, because the cooling air comes from the compressor. The mass flow rate of the cooling air is obtained from the pressure differences between the inside and outside of the transition piece.

Fourth, flow and heat transfer in the transition piece are calculated with film cooling. The mass flow rate of the film coolant, obtained from the results of the cooling channel analysis, is used in this step. The transition piece is modeled with film cooling holes in the cooling channel, and also near the picture frame. The film cooling holes near the picture frame are smaller than the other film cooling holes. They have a diameter of 1.38 mm, and there are 72 of them per side. The total number of grid cells in the transition piece with film cooling holes is 2.86 million.

Calculation of Wall Temperature and Thermal Stress

The wall adjacent temperatures and heat transfer coefficients on the inside and outside walls of the transition piece, obtained from the previous steps, are used to calculate the wall temperature. The wall temperature is then used to calculate the thermal stress. To calculate the wall temperature and thermal stress, the solid volume of the transition piece is modeled, and the total number of grid cells is 1.30 million for the solid volume. The commercial software ANSYS is used to calculate the wall temperature and thermal stress. When the thermal stress is calculated, a fixed boundary condition is imposed. According to the equation $\sigma = E\alpha\Delta T$, the thermal stress is proportional to the material properties. The body of the transition piece is made of Inconel 617. The material properties of Inconel 617 are summarized in Table 1 [8].

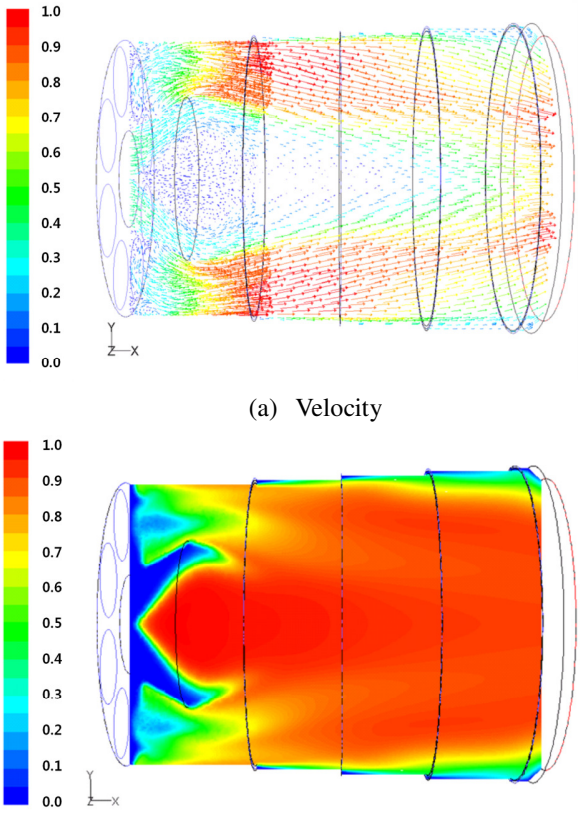

(a) Velocity

(b) Gas temperature

Figure 5. The velocity and gas temperature of the combustion gas in the combustion basket

RESULTS AND DISCUSSION

Combustion Basket Results

Figure 5 shows the results of combustion and flow analysis in the combustion basket. The velocity and temperature results are normalized by the maximum and minimum values. The air mixture, which had a vortical flow, entered the combustion basket from the nozzle. The velocity of the air mixture increased rapidly, and the flow structure was complex because of the combustion reaction. The recirculation region occurred near the center nozzle because of the vortical flow. The recirculation flow affected the flame stabilization in the gas turbine combustor. The velocity of the recirculation flow was relatively low. Thus, the velocities of the flow and the turbulent flame were equal in the recirculation region, and this phenomenon facilitated flame stabilization. Figure 6 shows the temperature distribution of the cross sections along the combustion basket. Figure 6(a) shows the temperature distribution and velocity vectors near the nozzle tip, including the vortices from all nine nozzles. The vortices rotated in the clockwise direction. Figure 6(b) shows the temperature distribution and velocity vectors near the center of the

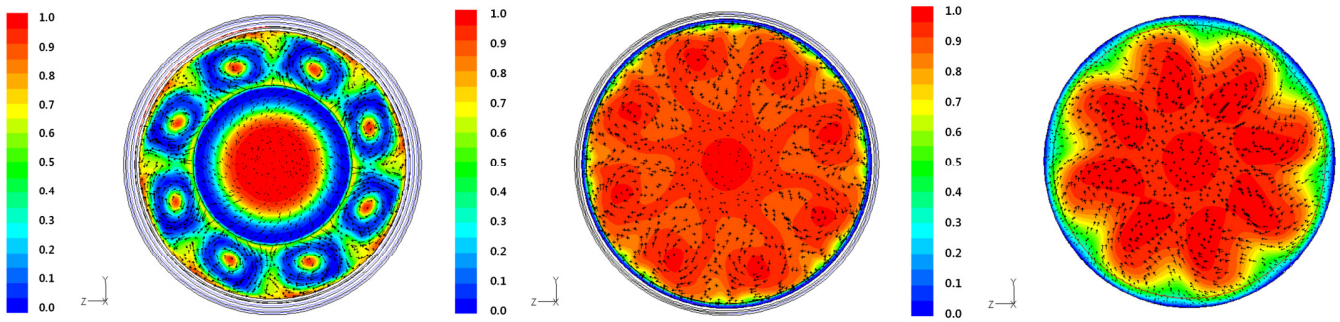

(a) Near the nozzle tip (b) Near the center (c) Near the outlet

Figure 6. Variation of swirls and gas temperature distribution along the combustion basket

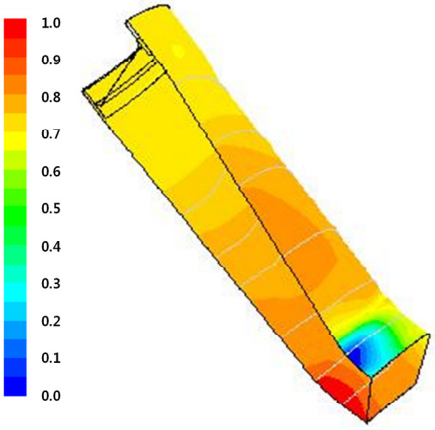

Figure 7. Static pressure distribution in the transition piece

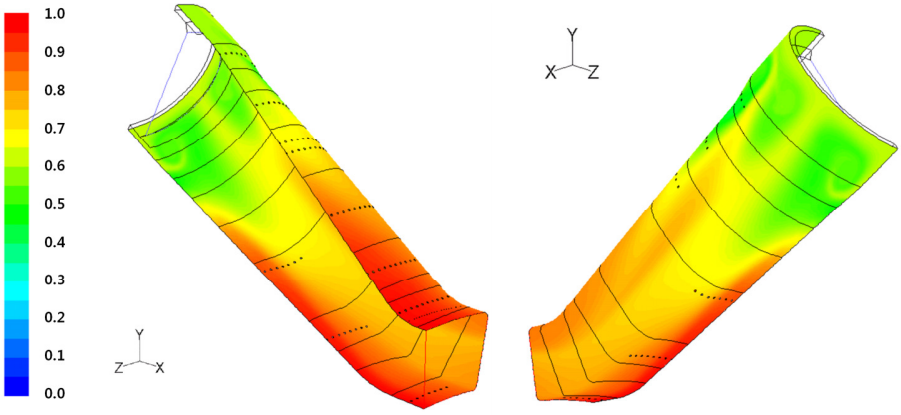

(a) Inside view (b) Outside view

Figure 8. Wall adjacent gas temperature on the transition piece without film cooling

combustion basket. In this region, all the vortices collided and were weakened. Nevertheless, the vortices increased the intensity of the turbulence, and facilitated uniform combustion. Figure 6(c) shows the temperature distribution and velocity vectors near the outlet of the combustion basket. Here, the vortices became weaker and were nearly dissipated. The temperature near the combustion wall was lower due to the coolant flow from the slot film cooling holes. The results for the outlet of the combustion basket, including the temperature distribution and velocity components, were applied to the inlet of the transition piece.

Pressure Distribution of the Transition Piece

As mentioned above, the pressure distribution of the transition piece must be calculated to obtain the mass flow rate of the cooling flow. To calculate the mass flow rate of the cooling flow, static pressures on both the inside and outside of the transition piece are required.

First, the static pressure on the inside of the transition piece was calculated. The static pressure distribution in the transition piece is shown in Fig. 7. The static pressure on the inside of the transition piece decreased from the inlet to the outlet, because the shape of transition piece was changed and the flow accelerated to the outlet.. In the turning region of the upper panel, near the end of the transition piece, the pressure was lower than in other regions, due to the flow detachment of turning flow. The hot gas flow is turned by the change in the shape of the transition piece. The hot gas separated by the turning effect, and the pressure near the turning region decreases. Figure 8 shows the wall adjacent temperature distribution of the transition piece. The temperatures on the upper and lower panels were higher than those on the sidewalls of the transition piece. The temperature increased and was uniform towards the outlet of the transition piece.

Second, the static pressure and heat transfer on the outside of the transition piece were calculated. Figure 9 shows the pressure distribution on the outside wall of the transition piece.

The compressed flow from the compressor collided with the lower panel of the transition piece. Accordingly, the pressure was high on the lower panel. The distribution of heat transfer coefficients on the outside of the transition piece was

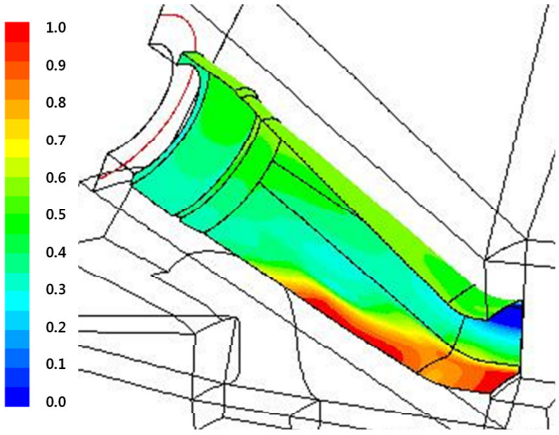

Figure 9. Static pressure distribution on the outside walls of the transition piece

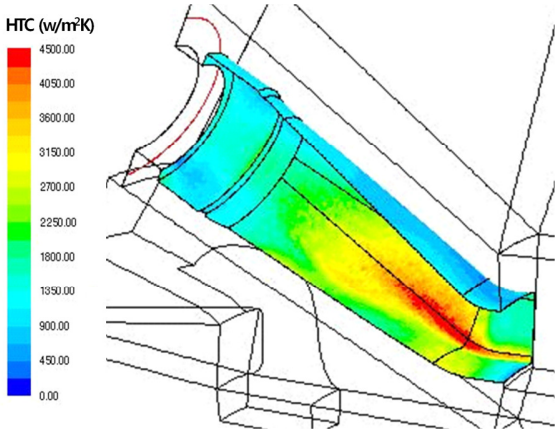

Figure 10. Heat transfer coefficient on the outside walls of the transition piece

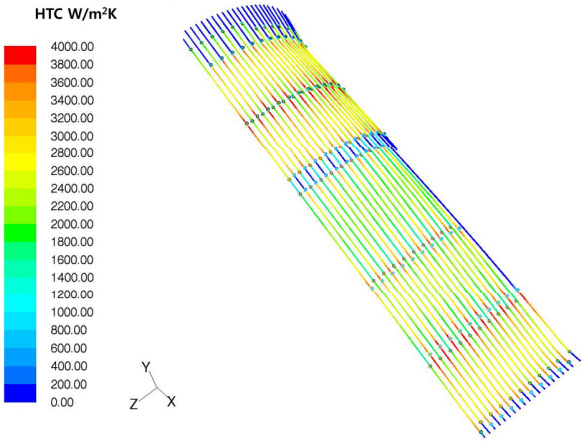

(a) Cooling channel on the upper panel

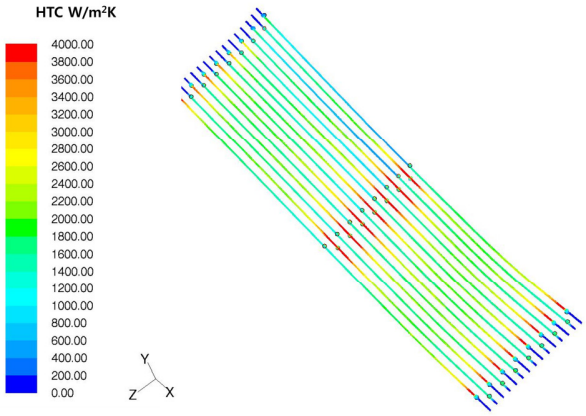

(b) Cooling channel on the lower panel

Figure 11. Heat transfer coefficients on the cooling channel

similar to the pressure distribution. Figure 10 shows the heat transfer distribution on the outside of the transition piece. The heat transfer coefficients were high on the lower panel, and low on the upper panel.

Heat and Flow Analysis in the Cooling Channels

Figure 11 shows the distribution of heat transfer coefficients in the cooling channels of the upper panel. The heat transfer coefficients were relatively high near the cooling holes. There was no flow in some channels, due to the structure and configuration of the channels, and these channels had very low heat transfer coefficients. The average velocity of the coolant flow was about 130 m/s, and the average value of the heat transfer coefficients was about 2,180 W/m^{2}K in the cooling channels of the upper panel. The flow and heat transfer distribution in the cooling channels of the lower panel were similar. The velocity range of the coolant flow was about 160 m/s, and the average value of the heat transfer coefficients was about 1,920 W/m^{2}K. The range of Reynolds numbers in the cooling channels were 60,000 ~ 80,000. The calculate values are similar to those of correlation in Eq. (4). Generally, the heat transfer coefficient in the circular channel is predicted by Eq. (4).

$$Nu = 0.023\, Re^{0.8} Pr^{0.3} \quad (4)$$

The correlation value of heat transfer coefficient calculated by Eq. (4) was 2,000 ~ 2,500 W/m^{2}K. It is similar to the results of present numerical analysis.

Heat and Flow Analysis in the Transition Piece with Film Cooling

Figure 12 shows the velocity vectors in the transition piece with film cooling. Recirculation flow occurred near the inlet of the transition piece. The wall adjacent gas temperature near the inlet was low because of the recirculation flow. The flow near

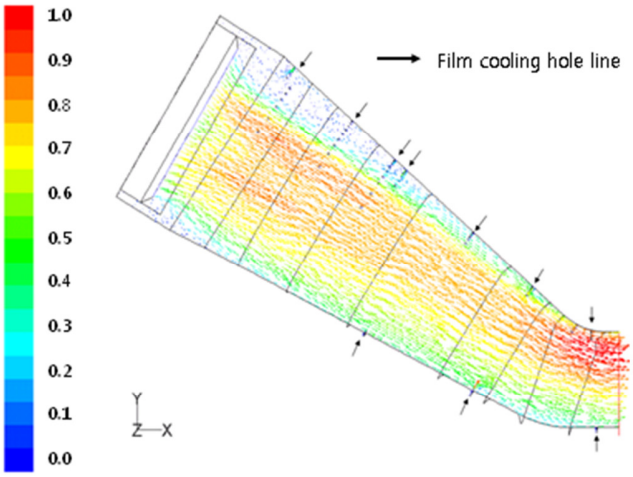

Figure 12. Flow velocity vectors in the transition piece

the inlet was deflected from the upper panel to the lower panel by the recirculation flow and film coolant. Thus, the wall adjacent gas temperature near the inlet was lower on the upper panel than on the lower panel.

The flow accelerated near the turning region, because the cross-sectional area of the transition piece decreased, and the flow was turned by the change in the shape of the transition piece. This raised the wall adjacent gas temperature near the upper panel of the transition piece.

The wall adjacent gas temperature in the transition piece was lower with film cooling than without it. The wall adjacent gas temperature behind the film cooling holes was low because the coolant covered the downstream region of cooling holes. In particular, the wall adjacent gas temperature was very low on the sidewalls of the transition piece and near the picture frame, due to the large quantity of film coolant in these areas. These results are shown the Fig. 13. The flow and wall adjacent gas

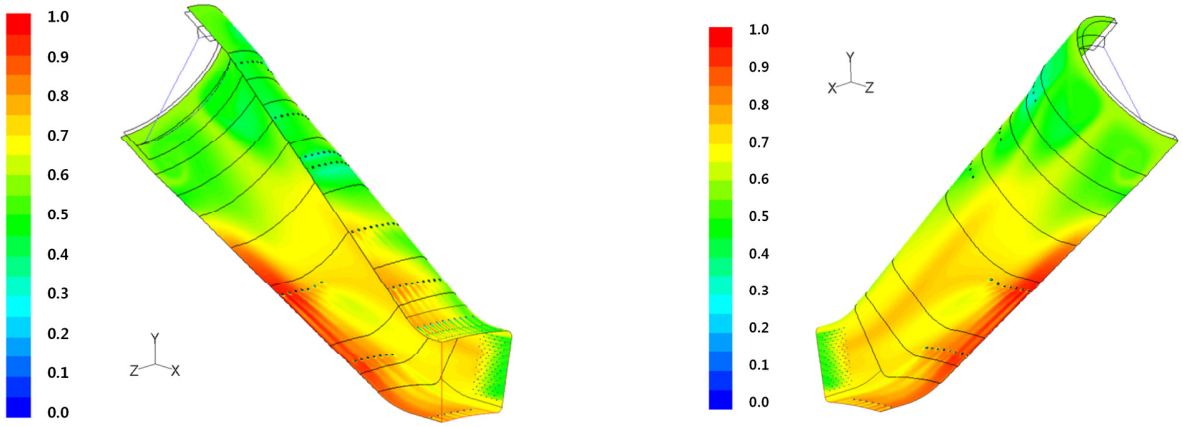

(a) Inside view (b) Outside view

Figure 13. The wall adjacent gas temperature distribution of the transition piece with the film cooling

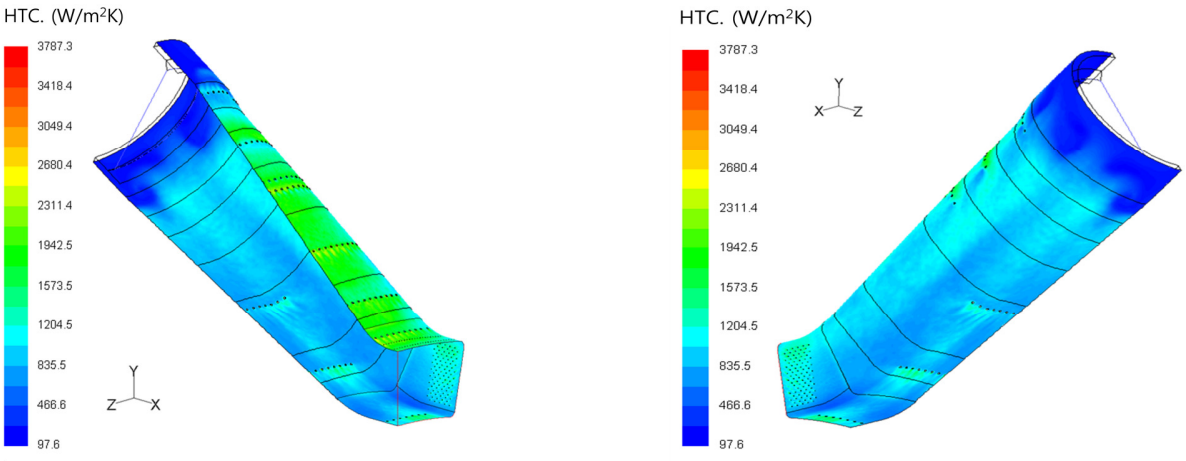

(a) Inside view (b) Outside view

Figure 14. Heat transfer coefficients on the transition piece

temperature distributions are reflected in the heat transfer distribution. The heat transfer coefficients were higher on the upper panel than on the lower panel. They were also high behind the film cooling holes. The distribution of the heat transfer coefficients on the transition piece with film cooling is shown in Figure 14. The average outlet gas temperature was about 1,570K. The difference between the calculated average value of the outlet gas temperature and the reference gas temperature (1,623K) was not significant.

Calculating the Wall Temperature and Thermal Stress on the Transition Piece

Figure 15 shows the temperature variation on the inner surface (the interface between the TBC coating and the base material) the base material (Inconel 617) of the transition piece. The range of temperatures on the TBC surface (which is directly exposed to hot combustion gas) was 719K to 1180K. The TBC coating protects the base material of the transition piece. Thus, the temperature was lower on the base material of the transition piece than on the TBC surface. The temperature on the inner surface of the base material of the transition piece ranged from 706K to 1,090K, and the temperature on the outside wall of the transition piece ranged from 667K to 1,030K. The TBC coating decreased the temperature by a maximum of 90K. Generally, the temperature was higher on the upper panel than on the lower panel. The upper panel had a broad high-temperature region, and the peak temperature region

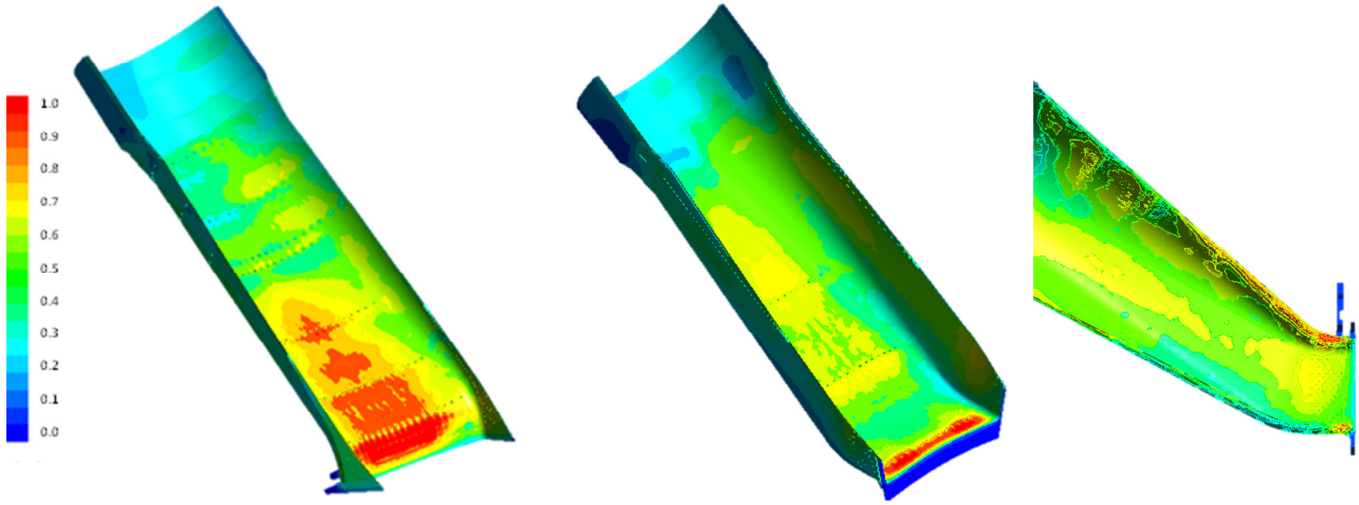

(a) Inside wall of the upper panel (b) Inside wall of the lower panel (c) Inside wall of the side wall

Figure 15. Wall temperature distribution on the inner surface of the base material of the transition piece

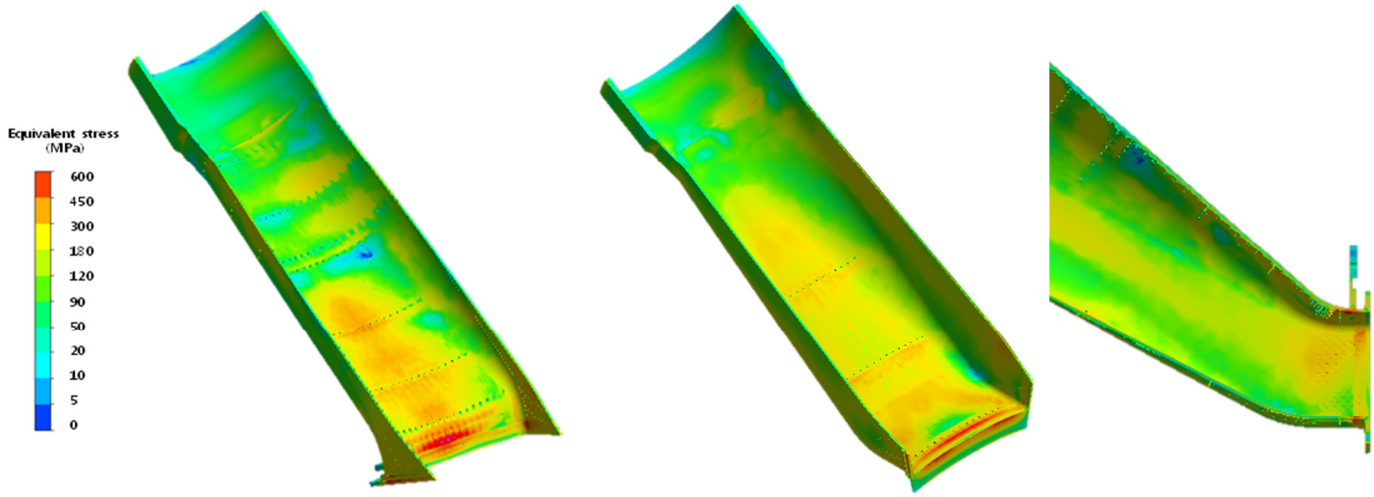

(a) Inside wall of the upper panel (b) Inside wall of the lower panel (c) Inside wall of the side wall

Figure 16. Thermal stresses distribution on the transition piece

(a) Failure of Lower panel (b) Crack on the corner region

Figure 17. Photos of the failure transition piece

.

was also on the upper panel. Compressed air from the compressor impinged to and cooled the lower panel of the transition piece. As a result, the wall temperature was lower on the lower panel than on the upper panel.

The peak temperature region was near the outlet wall on the upper panel, and was caused by the turning effect. High temperatures also occurred near the outlet wall on the lower panel. The temperature of the sidewalls of the transition piece was relatively low. Accordingly, the temperature gradient was steep in the corner regions between the upper/lower panels and the sidewalls.

Figure 16 shows the thermal stress distribution of the transition piece without TBC. The thermal stress was calculated from the wall temperature results, and was lower than that of other hot components of a gas turbine, such as the vanes and rotors. The range of thermal stress of the transition piece was 5.0 MPa to 650 MPa. The thermal stress distribution was in accord with the temperature distribution. The thermal stress on the transition piece increased from the inlet to the outlet. Peak and high temperature regions occurred on the upper and lower panel near the picture frame of the transition piece. The peak and high thermal stress also were occurred these regions. For the most part, when the temperature increased, the thermal stress also increased. Also, areas of high thermal stress occurred near the film cooling holes and the corner regions, due to the large temperature differences. Figure 17 is photos of the failure transition piece. The spallation of TBC coating and crack occur usually on the upper and lower panels near the picture frame (Fig. 17(a)) and the corner region (Fig. 17(b)), respectively. The spallation of TBC coating in Fig. 17(a) relates to the high temperature and thermal stress region in Figs. 15 and 16. However, the pattern of the crack in the corner region (Fig. 17(b)) relates rates to the high thermal stress region in Fig. 16(b). Therefore, the failure of transition piece is considered and predicted by both temperature and thermal stress distribution.

CONCLUSIONS

In this study, thermal analyses of a transition piece were conducted. The objective was to predict thermal damage and provide information for improving the efficiency and durability of transition piece of gas turbine. To this end, the combustion basket (liner), transition piece with cooling system, and dump diffuser were modeled. Flow and heat transfer in a transition piece were analyzed and creep life was predicted from the results of the flow and heat analysis.

To obtain the inlet conditions of the transition piece, the combustion field in the combustion basket was calculated. The pressure distributions on the inside and outside of the transition piece were calculated, and the mass flow rate of the coolant flow was derived from these. The flow and heat transfer were calculated in the cooling channels and the transition piece. The wall temperature was higher on the upper panel than on the other walls. The film coolant decreased the wall temperature near the film cooling holes. Thus, high temperature gradients occurred in the corner regions and near the film cooling holes. These high temperature gradients induced high thermal stresses.

The upper panel had high wall temperatures and thermal stresses, and minimum lifetime. This region is vulnerable to thermal effects, and the cooling system needs to be improved on the upper panel of the transition piece. These results provide basic data for designing the cooling system of a transition piece, and for facilitating its maintenance. With the help of this information, it will be possible to upgrade the efficiency and durability of the transition pieces.

NOMENCLATURE

E	Young's modulus
P	Larson – Miller parameter
T	Temperature
t_r	Time to rupture
α	Thermal expansion
σ	Equivalent stress
σ_r	Rupture stress

REFERENCES

[1] Kim, W. W., Menon, S., and Mongia, H. C., 1999, "Large-Eddy Simulation of a Gas Turbine Combustor Flow", Combustion Science and Technology, Vol. 143, pp. 25-62.

[2] Chung, J. H., Seo, S. B., Ahn, D. H., and Kim, J. J., 2000, "Numerical Analysis of the Flow Characteristics in a Lean Premixed Gas Turbine Combustor for Power Generation", Proceeding of KSME Vol. 1 (2), pp. 847-852.

[3] Kang, S., Kim, Y., Chung, J. H. and Ahn, D. H., 2005, "Numerical Modeling for Flame Stabilization of A Lean-Premixed Gas Turbine Combustor", Proceeding of KSME, pp. 1908-1914.

[4] Agrawal, A. K., Kapat, J. S., and Yang, T. T., 1998, “An Experimental /Computational Study of Airflow in the Combustor-Diffuser System of a Gas Turbine for Power Generation", ASME, Vol. 120, pp. 24-33.

[5] Bailey, J. C., Intile, J., Fric, T. F., Tolpadi, A. K., Nirmalan, N. V., and Bunker, R. S., 2003, “Experimental and Numerical Study of Heat Transfer in a Gas Turbine Combustor Liner", Journal of Engineering for Gas Turbines and Power, Vol. 125, pp. 994-102.

[6] Mustafa, A. H., Mashmi, M. S. J., Yilbas, B. S., and Sunar, M., 2006, “Thermal stress analysis in annular duct resembling gas turbine transition piece”, Journal of Materials Processing Technology, Vol. 171, pp. 285-294.

[7] Larson, F. R., and Miller, James, A Time-Temperature Relationship for Rupture and Creep Stresses, Trans. ASME, Vol.74, 1952 pp. 765–775.

[8] Smith. G.D., and Yates. D. H., “Optimization of the Fatigue Properties of INCONEL alloy 617”,ASME Paper No. 91-GT-16.